Erythrocyte aggregation tendency and cellular properties in horse, human, and rat: a comparative study

OGUZ K. BASKURT, ROBERT A. FARLEY, AND HERBERT J. MEISELMAN
Department of Physiology and Biophysics, University of Southern California School of Medicine, Los Angeles, California 90033

Baskurt, Oguz K., Robert A. Farley, and Herbert J. Meiselman. Erythrocyte aggregation tendency and cellular properties in horse, human, and rat: a comparative study. *Am. J. Physiol.* 273 (*Heart Circ. Physiol.* 42): H2604–H2612, 1997.—Horse blood has a higher tendency to form red blood cell (RBC) aggregates compared with human blood, with this enhanced aggregation previously attributed to differences in plasma factors. Our results confirm this observation and further indicate that washed horse RBC also have a significantly higher aggregation tendency in dextran 70 solutions (i.e., horse RBC have a higher "aggregability"). In contrast, the aggregation tendency of rat RBC, both in autologous plasma and in dextran 70, is significantly less compared with human and horse RBC. Other rheological findings for horse and rat RBC include smaller changes in RBC deformation indexes over the same shear stress range and a lower RBC shape recovery time constant. Rat RBC also had higher two-phase aqueous polymer partition coefficients, suggesting a higher surface charge. Membrane protein analysis by sodium dodecyl sulfate-polyacrylamide gel electrophoresis revealed marked differences: *1*) *band 4.2* protein was lacking in horse RBC membranes, and *2*) carbohydrate groups have different distributions in human, rat, and horse RBC, as indicated by different patterns in periodic acid-Schiff-stained protein bands. Our results clearly indicate significant differences in RBC aggregability among the three species and indicate that cellular factors contribute importantly to these differences. Furthermore, they suggest that systematic studies of blood and RBC from different species should provide insight into the mechanism(s) of RBC aggregation.

red blood cell aggregation; hemorheology

INVESTIGATION OF THE rheological properties of blood from various species has attracted considerable interest, and comparative hemorheology studies have yielded interesting, even surprising, findings about the flow behavior of blood. It has been observed that the rheological properties of blood can differ markedly between species, although the basic structure of their blood is relatively similar (17). In all mammals, blood is composed of hemoglobin-carrying red blood cells (RBC) and a small amount of white blood cells (WBC) suspended in plasma; the volume percentage of RBC in the blood (hematocrit) is nominally between 30 and 50% (21). In almost all mammals, RBC are biconcave disks under normal physiological conditions, whereas their mean size may differ between species (17, 21).

Previous reports have indicated that both the cellular deformability (2, 4, 46) and the aggregation characteristics (23, 32, 33) of mammalian RBC exhibit a wide range among various species. This variation is also reflected by viscometric measurements on mammalian blood from various sources (21, 42, 48). It is obvious from the current literature that the size of the animal as well as the size of their RBC are not the only determinants of hemorheological behavior (18, 33). Although plasma composition has been found to differ among species, this factor alone does not provide a satisfactory explanation for the hemorheological variations (42). Popel et al. (33) related the degree of aggregation in different species to their exercise capacity and found it to be higher in athletic species. Studies by Meiselman et al. (28) on seal blood revealed very different RBC aggregation characteristics between two species of seals living near the North and South Poles. Despite these and other investigations, a clear understanding of the "logic" behind the hemorheological variations among mammals has not yet been established, nor has the physiological significance of these hemorheological differences been clearly defined (14). However, RBC aggregation has been shown to affect venous vascular resistance and has been suggested to play a role in determining microcirculatory hemodynamics (9).

Comparative hemorheology studies may also yield valuable information relevant to the structural bases of RBC rheological behavior. It has been shown by several studies that cellular properties play an important role in RBC aggregation (6, 27, 31). Despite the more clearly understood structural aspects of RBC deformability (12, 29), information about the cellular determinants of RBC aggregation is limited (34). A detailed, systematic analysis of RBC structure in various species, and the relations between these findings and RBC aggregation characteristics, may possibly provide more appropriate models of RBC aggregation.

In the present study, the aggregation behavior and associated structural and biophysical properties of horse, human, and rat RBC were investigated, with a special emphasis on the role of cellular factors in RBC aggregation. That is, this study was focused on RBC "aggregability" as a cellular property, rather than on RBC aggregation, which reflects the combined influence of cells, suspending medium, and flow conditions (27). Selection of these three mammalian species was based on distinct differences in their RBC aggregation characteristics (23, 27, 32, 33): *1*) horse RBC in plasma exhibit an intense aggregation tendency; *2*) the aggregation tendency of rat RBC in plasma is very weak; and *3*) the aggregation behavior of RBC in normal adult human blood is intermediate between these two extremes (27). In addition, extensive hemorheological data exist for humans (e.g., see Ref. 25), and thus the use of blood from hematologically normal adult human donors provides "baseline" data for comparison with other mammals.

0363-6135/97 $5.00 Copyright © 1997 the American Physiological Society

Downloaded from http://ajpheart.physiology.org/ by 10.220.33.1 on October 18, 2017

MATERIALS AND METHODS

Blood sample collection and preparation. Horse blood samples, withdrawn from the jugular vein, were obtained from healthy 3- to 6-yr-old various-breed horses of either gender. Rat blood was obtained from Swiss-Albino rats weighing 300–350 g by abdominal aorta puncture after laparatomy under pentobarbital sodium anesthesia (25 mg/kg body wt). Human blood was obtained from healthy adults, age range of 28–54 yr and of either gender. All blood samples were withdrawn into sterile vacuum tubes and anticoagulated with EDTA (1.5 mg/ml blood). All analyses were completed within 4 h after the collection of blood samples.

The hematocrit of a portion of each blood sample was adjusted to 40% either by removing or adding autologous plasma. The remaining portion was centrifuged at 1,400 *g* for 6 min, the plasma was removed, and the RBC were washed three times in isotonic phosphate-buffered saline (PBS; pH = 7.4, 290 mosmol/kgH_2O). The RBC were then resuspended at 40% hematocrit in isotonic dextran 70-PBS solutions or used for other measurements as described below. Dextran 70 (70,000 molecular weight) was obtained from Sigma Chemical (St. Louis, MO) and was used at a concentration of 3% (wt/vol) unless otherwise stated.

Assessment of RBC aggregation. RBC aggregation was quantified using a photometric rheoscope (Myrenne Aggregometer; Myrenne, Roetgen, Germany) interfaced to a digital computer. This technique is based on the increase of light transmission through an RBC suspension that occurs when individual cells aggregate; gaps in the suspending medium between the aggregates allow more light to pass through the suspension. Two indexes of RBC aggregation were determined with the Myrenne system as described previously (7): *1*) "M," which is measured by integrating light transmission for 10 s, at stasis, immediately after a brief period of high shear (600 s^{-1}) to disrupt previously existing aggregates and *2*) "M1," which is measured by integrating light transmission for 10 s, at a low shear rate of 3 s^{-1}, immediately after the period of high shear. Note that M thus reflects aggregation in the absence of shear, and M1 reflects aggregation when fluid movement tends to promote cell-to-cell interaction; both M and M1 increase with increasing RBC aggregation (27, 34). RBC aggregation was measured in autologous plasma or in PBS-dextran 70 solutions. All Myrenne studies were carried out at 40% hematocrit and at room temperature (22 ± 1°C).

RBC aggregation was also evaluated by the zeta sedimentation rate (ZSR) method of Bull and Brailsford (8). Well-mixed RBC suspensions were drawn into 2-mm ID glass tubes, placed in a Zetafuge (Coulter Electronics, Hialeah, FL), and rotated with the axis of the tubes in a nearly vertical position for four 45-s periods. The hematocrit of the suspension after the 3-min period is termed the Zetacrit, and the ZSR is calculated as the ratio of the true hematocrit (13,000 *g* for 4 min) to the Zetacrit. Note that, like M and M1, the ZSR is higher with higher degrees of RBC aggregation and that, in the absence of aggregation, ZSR = 0.40 for a 40% hematocrit suspension.

Viscosity measurements. The apparent viscosities of RBC suspensions in autologous plasma or in 3% dextran 70 at a hematocrit of 40% were measured using a Couette viscometer (Contraves LS 30; Contraves, Zurich, Switzerland) at shear rates between 0.512 and 94.5 sec^{-1}. For some experiments, the viscosities of RBC suspensions were also measured at higher shear rates (300–1,500 s^{-1}) with a rotational cone-plate viscometer (model 1/2 RVT-200; Brookfield Engineering Laboratories, Stoughton, MA). All viscosity studies were carried out at 25°C.

Measurement of RBC deformability. RBC deformability (i.e., the ability of the entire cell to adopt a new shape in response to deforming forces) was determined, at fluid shear stresses between 0.5 and 50 Pa, by laser diffraction analysis using an ektacytometer (LORCA; RR Mechatronics, Hoorn, The Netherlands). The system has been described elsewhere in detail (19). Briefly, the sample is sheared in a concentric-cylinder Couette system made of glass, with a gap of 0.3 mm between the cylinders; the laser light beam is passed through the sample perpendicular to the shear plane. The shape of the diffraction patterns resulting from RBC deformation is analyzed by a microcomputer, and elongation indexes (EI) are calculated; an increased EI indicates greater cell deformation and hence greater cell deformability. For these LORCA studies, the RBC were suspended in an isotonic, viscous (24.8 mPa·s) PBS-dextran 70 solution (≈20% wt/vol dextran 70) at a cell count of 2×10^7/ml; all measurements were carried out at 25°C.

Determination of RBC shape recovery time constant. RBC were suspended in an isotonic, viscous (10 mPa·s) PBS-dextran 40 (40,000 molecular weight; Sigma) solution at a hematocrit of 40% and were tested at 25°C as previously described (5). The RBC suspension was sheared at 500 s^{-1} for 10 s in the LORCA-Couette system described above, after which the shear rate was abruptly reduced to zero. Laser light reflectance from the RBC suspension after this sudden stop of the outer cylinder was measured by photodiodes built into the inner cylinder and was digitized by computer at a sampling rate of 500 Hz. The first 400-ms portion of the data was transferred to data analysis software (Statmost; Datamost, Salt Lake City, UT) for curve fitting. An exponential equation ($I = I_\infty - I_d \cdot e^{-t/t_c}$) was fitted to the light reflectance-time data, and the time constant (t_c) was calculated using a least-square minimization technique. The term t_c is the time constant for RBC shape recovery after the abrupt removal of the deforming shear force, with a decreased t_c indicating a faster rate of shape recovery.

Determination of RBC partition coefficient. RBC partition coefficients were determined at room temperature (22 ± 1°C) by a two-phase aqueous system containing 5% dextran 500 (500,000 molecular weight; Pharmacia Fine Chemicals, Uppsala, Sweden) and 4.3% polyethylene glycol (PEG; 8,000 molecular weight; Sigma) in isotonic phosphate buffer (pH = 6.8). The two polymers were dissolved in the phosphate buffer; the phases were allowed to form, separate, and equilibrate for 24 h; and then each phase (dextran-rich bottom, PEG-rich top) was harvested and frozen until use. Packed RBC (30 μl) were added to tubes containing 1.5 ml of each phase, and the contents of the tubes were mixed well by repeated inversion. After mixing, the phases were allowed to reform and separate for 20 min. The hemoglobin concentration in the top phase was measured spectrophotometrically at 538 nm after lysing the RBC in Drabkin's reagent, and the partition coefficient was calculated as the ratio of hemoglobin content of the top phase to the total hemoglobin in the 30 μl of packed RBC. Note that, because the two-phase system used for these measurements is "charge sensitive," a lower partition coefficient indicates a decreased RBC surface charge (43).

RBC membrane protein electrophoresis. RBC membrane proteins were separated by sodium dodecyl sulfate (SDS)-polyacrylamide gel electrophoresis (PAGE) according to Laemmli (24). RBC ghosts were prepared by hypotonic lysis, and 60 μg of protein samples were solubilized in SDS-phosphate buffer solution and loaded onto 10% polyacrylamide gels. Electrophoresis was carried out for 18 h at 4°C with a constant voltage of 80 volts. The gels were then stained with either Coomassie brilliant blue or the periodic acid-

Downloaded from http://ajpheart.physiology.org/ by 10.220.33.1 on October 18, 2017

Table 1. *Hematological values for horse, human, and rat blood samples*

	Horse ($n = 6$)	Human ($n = 6$)	Rat ($n = 6$)
WBC, 10^9/l	7.31 ± 0.48	6.16 ± 0.48*	5.88 ± 0.56‡
RBC, 10^{12}/l	8.68 ± 0.508	4.52 ± 0.19†	7.54 ± 0.17*§
Hemoglobin, g/l	154.4 ± 10.7	136.8 ± 6.7	145.5 ± 1.7
Hematocrit, l/l	0.42 ± 0.02	0.40 ± 0.02	0.42 ± 0.006
MCV, fl	48.50 ± 0.69	89.16 ± 2.16†	56.51 ± 0.76†§
MCHC, g/l	364.5 ± 4.1	339.0 ± 4.4†	347.5 ± 2.1†

Values are means ± SE; *n*, no. of subjects. WBC, white blood cell count; RBC, red blood cell count; MCV, mean corpuscular volume; MCHC, mean cellular hemoglobin concentration. Difference from horse: *$P < 0.05$ and †$P < 0.01$. Difference from human: ‡$P < 0.05$ and §$P < 0.01$.

Schiff reaction (16), and the dried gels were quantitatively scanned to determine protein composition.

Miscellaneous techniques. Hemoglobin and hematocrit values, RBC and WBC counts, and RBC mean corpuscular volume (MCV) were obtained using an electronic hematology analyzer (Helios; Roche Diagnostic Sysyems, Branchburg, NJ). RBC counts in the suspensions used in the LORCA were also adjusted using this analyzer. The osmolality of solutions was determined by a freezing-point depression osmometer (model 5004; Precision Systems, Natick, MA) and pH by an Orion model 410A system (Orion Research, Boston, MA). The viscosities of the dextran solutions used in ektacytometry were measured at 25°C by a cone-plate viscometer (model 1/2 RVT-200; Brookfield Engineering Labs, Stoughton, MA).

Statistics. Results are expressed as means ± SE unless otherwise stated.

RESULTS

Hematology. Hematological parameters for horse, human, and rat blood samples are presented in Table 1. Hematocrit values in all three species were ~0.4 l/l (40%), although RBC counts in horse and rat blood were considerably higher than human samples; the reason for this difference is the much smaller MCV of horse and rat RBC. Total hemoglobin levels were highest in horse blood and lowest in human blood, and mean cellular hemoglobin concentration (MCHC) values were also higher in horse blood compared with the human and rat samples.

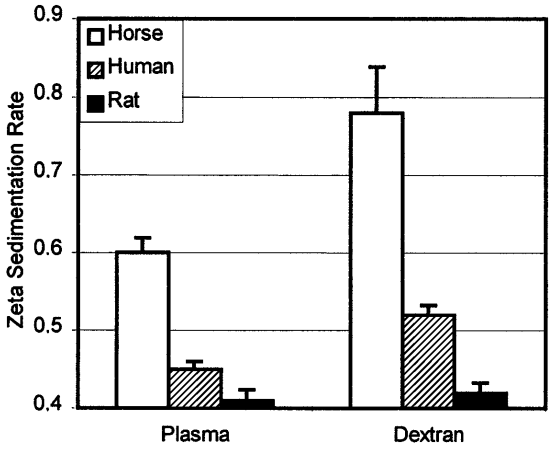

Fig. 2. Zeta sedimentation rates in autologous plasma or in 3% dextran 70 for RBC from horse, human, and rat blood. Values are means + SE; $n = 6$ in each group.

RBC aggregation In autologous plasma, RBC aggregation was markedly greater for horse RBC at both stasis (M) and under low shear (M1) compared with human RBC (Fig. 1). In contrast, rat RBC exhibited a very slight degree of aggregation, with the ratio of horse to rat aggregation parameters being ~18-fold for M and 10-fold for M1. M1 indexes for RBC suspended in 3% dextran 70 showed a similar pattern, being highest for horse RBC and lowest for rat RBC (Fig. 1). However, M indexes in 3% dextran 70 for horse and human RBC were almost identical; there was no detectable aggregation at stasis (M mode) for rat RBC in dextran (Fig. 1). ZSR measured in either autologous plasma or in 3% dextran 70 indicated a similar trend for RBC aggregation: horse > human > rat (Fig. 2).

The above results using a fixed 3% dextran 70 concentration were based on previous studies with human RBC that demonstrated maximal aggregation at this concentration of dextran (31). However, our experiments with RBC suspensions prepared using

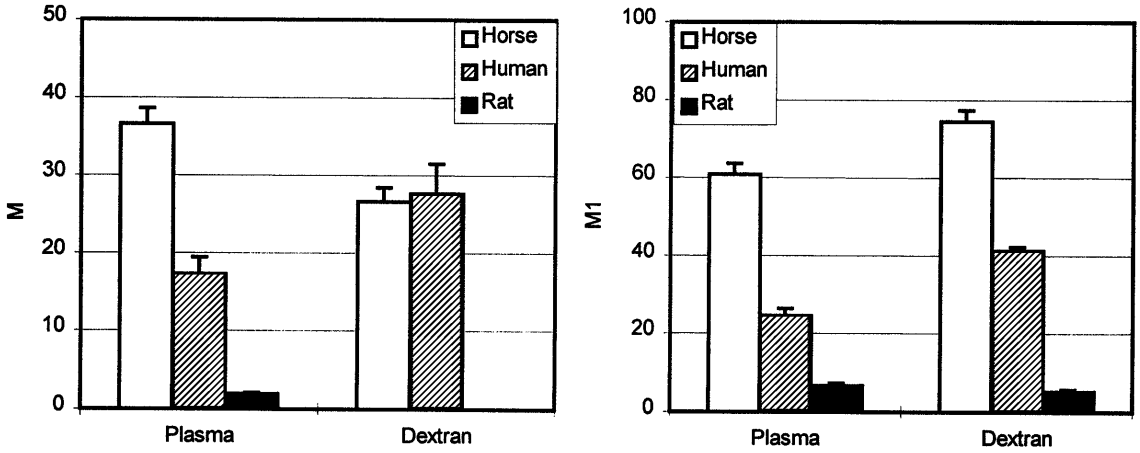

Fig. 1. M (*left*) and M1 (*right*) aggregation indexes measured in autologous plasma or in 3% dextran 70 for red blood cells (RBC) from horse, human, and rat blood. M indexes for rat RBC in 3% dextran 70 were too low to be measurable. Values are means + SE; $n = 6$ in each group. Note that M and M1 ordinate scales differ by a factor of 2.

Downloaded from http://ajpheart.physiology.org/ by 10.220.33.1 on October 18, 2017

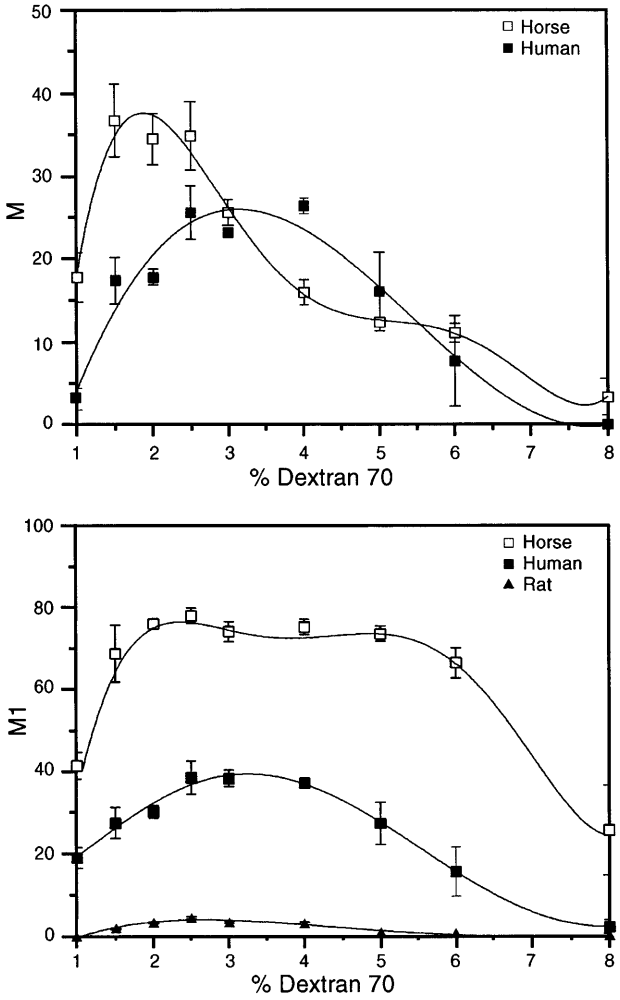

Fig. 3. Concentration dependence of aggregation indexes (M and M1) for horse, human, and rat RBC suspended in various concentrations of dextran 70. M indexes for rat RBC were not measurable in any of the concentrations. Values are means ± SE of 5 experiments. Curves are 5th-order polynomials for horse data and 3rd-order polynomials for human and rat data.

various dextran concentrations (1–8%) clearly indicated that the RBC aggregation response to dextran concentration differs between the three species: *1*) horse RBC aggregation at stasis (M value) reaches a peak value at a dextran concentration of ~2% (Fig. 3), and, at this concentration, horse RBC aggregation was about twofold higher than for human RBC; *2*) peak aggregation for horse RBC in 2% dextran was also higher (≈40%) than the peak aggregation for human RBC in 3% dextran, whereas, in 3% dextran, M aggregation indexes were the same for horse and human RBC. These latter results thus confirm the data presented in Fig. 1 (i.e., equal M values for horse and human RBC in 3% dextran), which were obtained using a separate set of samples. At dextran concentrations ≥5% there were no meaningful differences between horse and human RBC. Aggregation under low shear (M1) also tended to reach a maximum at a lower dextran concentration for horse versus human RBC, with aggregation in dextran always markedly higher for horse RBC regardless of dextran concentration (Fig. 3). The shape of the dextran concentration-M1 curve for horse RBC is obviously different from that for human RBC in that it has a plateau between 2 and 5% dextran, whereas the curve for human RBC is bell shaped with a maximum at 3%. The rat RBC M1 data also suggest a plateau between 2 and 4% (Fig. 3).

Suspension viscosity. The apparent viscosities of RBC suspended in autologous plasma or in 3% dextran 70 were measured for all three species over a wide range of shear rates (Fig. 4). At shear rates >28 s^{-1} the viscosities of the suspensions were essentially identical. Below this shear rate, horse RBC suspensions in either plasma or dextran had the highest viscosity, with the difference between horse and human or rat samples becoming larger with decreasing shear rate. At a shear rate of 0.512 s^{-1} the viscosity of horse RBC suspensions in autologous plasma was ~70% higher than for human RBC in plasma; a similar pattern (i.e., horse > human > rat) was also observed for RBC suspended in dextran. It is interesting to note that, at shear rates <10 s^{-1}, rat RBC suspended in autologous plasma had slightly higher viscosities compared with human RBC, whereas, for the dextran suspensions, rat RBC exhibited nearly identical viscosities, except at the lowest rate of shear.

RBC deformability. Figure 5 presents RBC deformability data, as EI values measured via laser ektacytometry (i.e., LORCA system), for horse, human, and rat RBC. At very low shear stresses, EI for human RBC was the lowest, and the EI of rat RBC was the highest.

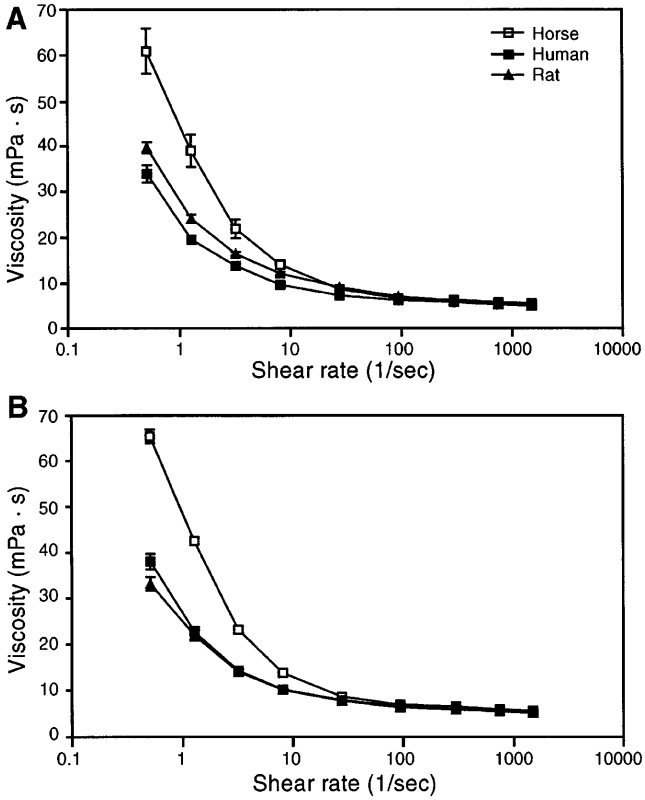

Fig. 4. Viscosity of RBC suspensions as function of shear rate for RBC in autologous plasma (*A*) and in 3% dextran 70 solution (*B*). Hematocrit of all suspensions was 40%. Values are means ± SE; n = 6 in each group.

Downloaded from http://ajpheart.physiology.org/ by 10.220.33.1 on October 18, 2017

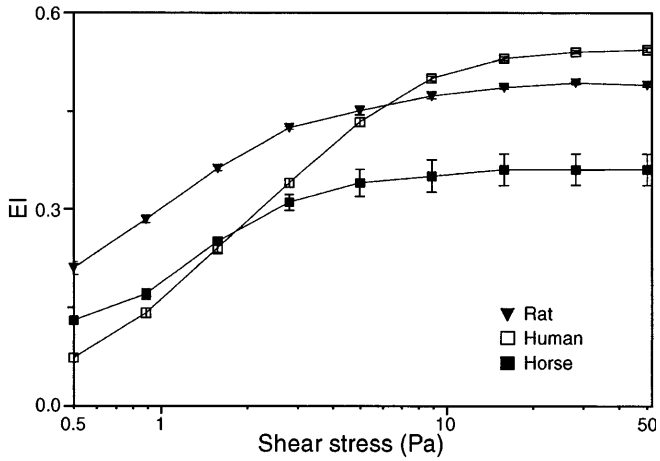

Fig. 5. Ektacytometer elongation indexes (EI) versus fluid shear stress for horse, human, and rat RBC. Values are means ± SE; $n = 6$ in each group.

However, with increasing shear stress, EI for human RBC increased most rapidly (i.e., greater slope), indicating a greater deformation response to the applied shear stress. For human RBC, EI increased almost eightfold as the shear stress increased from 0.5 to 50 Pa, whereas the increment under the same conditions was ~3-fold for horse RBC and 2.3-fold for rat RBC. Note that both horse and rat RBC reached their limiting, maximal deformation at lower shear stresses than human RBC. There was high interindividual variation for EI in horse samples as indicated by the large error bars shown in Fig. 5. This difference in variation between species was especially obvious at shear stresses >5 Pa: the coefficient of variation at 28 Pa was 16.6% for horse RBC, 1.3% for human RBC, and 1.1% for rat RBC.

Another indicator of differences in RBC rheological behavior among the three species was the RBC shape recovery t_c. As shown in Fig. 6, horse RBC had a lower t_c (i.e., a faster shape recovery process) versus either human or rat RBC. Inasmuch as the RBC t_c is proportional to the ratio of membrane surface viscosity to membrane shear elastic modulus (5), these results thus indicate a marked decrease of this ratio for horse RBC.

RBC physicochemical properties. RBC two-phase aqueous partition coefficients, which can reflect variations of charge-associated surface properties (43), exhibited large differences among the three species studied: lowest for horse RBC, intermediate for human RBC, and highest for rat RBC (Fig. 7). Thus these partition coefficients suggest the following order for RBC surface charge: rat > human > horse.

Figure 8 summarizes the results of SDS-PAGE analysis of RBC membrane proteins. The major membrane protein bands stained by Coomassie blue, including *bands 1*, *2*, *3*, and *5*, were present in RBC from all three species and appear to have almost identical molecular weights. Although two separate bands (4.1 and 4.2) were clearly evident at the beginning of the *band 4* region for human and rat RBC, the presence of more than one band in this region of horse RBC is not obvious. *Band 6* was only observed in human samples and was lacking in horse and rat RBC.

Gels run simultaneously with the Coomassie blue-stained gels, but stained by the periodic acid-Schiff reaction to show carbohydrate-rich proteins, revealed several distinct patterns in the three species. As shown in Fig. 8, the major carbohydrate-rich protein in human RBC appears to have a molecular weight that is almost coincident with *band 3* (i.e., 95,000); two minor bands were also present with molecular weights of ~71,000 and 40,000. In horse RBC membranes, carbohydrate-rich proteins seem to be distributed within two bands: the first one has a molecular weight of ~75,000, and the second appears to be ~30,000. Two separate carbohydrate-rich bands also appeared in rat RBC membrane samples, with molecular weights of ~84,000 and 36,000.

DISCUSSION

The greatly enhanced tendency for RBC aggregation in horse blood is well known, has been partially ascribed to the higher molecular weight of horse fibrino-

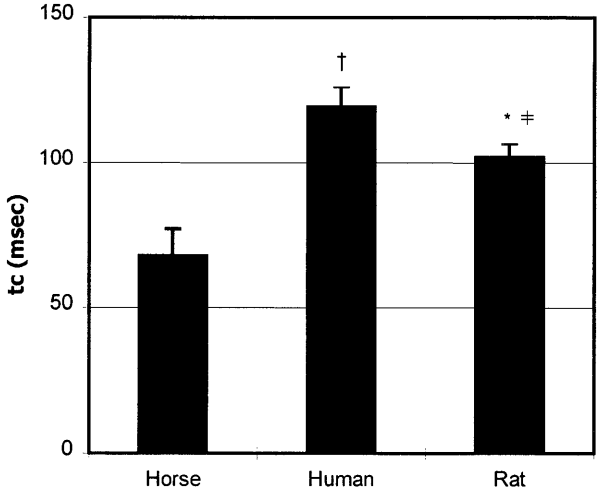

Fig. 6. Shape recovery time constant (t_c) of horse, human, and rat RBC. Values are means + SE; $n = 6$ in each group. Difference from horse: $*P < 0.05$ and $\dagger P < 0.01$. Difference from human: $\ddagger P < 0.05$.

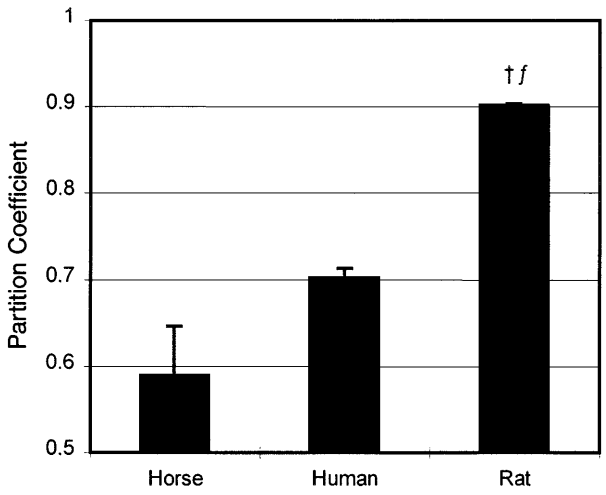

Fig. 7. Two-phase aqueous partition coefficients for horse, human, and rat RBC. Values are means + SE; $n = 6$ in each group. Difference from horse: $\dagger P < 0.01$. Difference from human: $^f P < 0.01$.

Downloaded from http://ajpheart.physiology.org/ by 10.220.33.1 on October 18, 2017

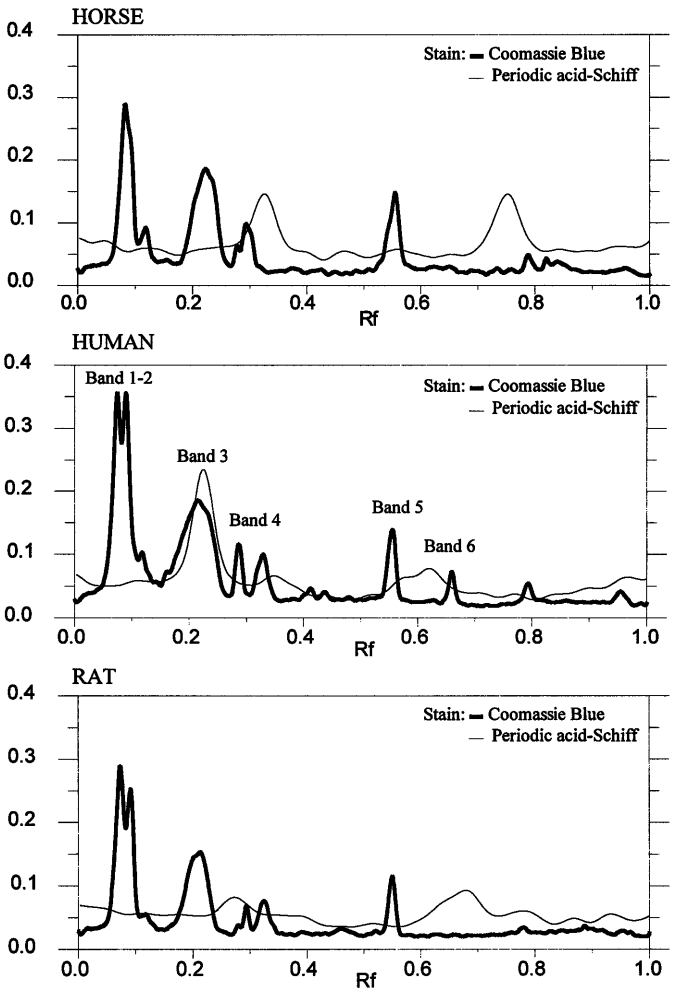

Fig. 8. SDS-polyacrylamide gel electrophoresis analysis of membrane proteins from horse, human, and rat RBC, stained by Coomassie blue and periodic acid-Schiff reaction. R_f is relative mobility, whereas the *y*-axis represents the optical density of protein bands in arbitrary units. Labels shown for humans refer to the Coomassie blue-stained gels.

gen (3), and has been detailed by previous reports (23, 33). Different methods have been used to assess RBC aggregation in horse blood, including RBC sedimentation rate measurements (1, 33), photometric methods (23), and viscometric techniques. Viscometric data for horse blood indicate high apparent viscosity values at low rates of shear (3, 33, 48), and, because enhanced RBC aggregation is known to elevate the low shear rate viscosity of blood (34), these data also support the observations of elevated RBC aggregation in horse blood. Our results related to horse RBC aggregation in autologous plasma (Figs. 1, 2, and 4) are thus in agreement with previous reports in that we observed higher photometric aggregation indexes (M and M1), a higher ZSR, and higher low shear viscosity for horse RBC versus either human or rat RBC. Conversely, rat RBC were characterized as having the lowest aggregation tendency, as evidenced by very low photometric aggregation indexes and a low ZSR; however, low shear viscometry results for rat RBC in autologous plasma indicated slightly higher values versus human RBC (Fig. 4).

Although our findings for RBC aggregation in horse versus human blood are consistent with prior reports, our results for RBC aggregation in human versus rat blood are not in agreement with the data presented by Ohta et al. (32), who indicate similar RBC aggregation for rat and human blood. This discrepancy in findings is potentially related to methodological differences: Ohta et al. also used a photometric method but quantitated aggregation during tube flow rather than in a system such as the Myrenne Aggregometer in which the shear field between the cone and plate can be well controlled and well defined (7). Furthermore, it has been previously confirmed that the Myrenne Aggregometer system used herein (7) is capable of measuring RBC aggregation in rat blood and that it can detect enhanced RBC aggregation in blood from septic rats (6). These findings (6) thus exclude the possibility of the Myrenne system being insensitive to RBC aggregation in rat blood due to specific rat RBC properties (e.g., cell geometry). In addition, the low aggregating tendency of rat blood versus human blood was demonstrated by the ZSR method (Fig. 2), which does not employ photometric measurement techniques (8). Although our low shear viscometry results (Fig. 4) do seem to suggest similar RBC aggregation for rat and human blood, note that it has been suggested that low shear apparent viscosity may not always solely reflect RBC aggregation, especially for differing RBC mechanical or geometric properties (26).

On the basis of our current data as well as the vast majority of previous literature reports, it is clear that RBC aggregation in plasma differs among the three species studied herein, with the order of aggregation tendency being horse > human > rat. Moreover, the aggregation tendencies for washed RBC resuspended in a defined and constant dextran 70 solution (i.e., RBC aggregability) also tend to follow the same pattern of horse > human > rat (Figs. 1 and 2). Thus these results for aggregation in plasma and dextran both confirm and extend our prior observations (27, 31, 38): in addition to suspending medium properties (e.g., plasma protein levels, polymer concentration and physicochemical characteristics), RBC cellular factors are important determinants of RBC aggregation behavior.

It is well known that the extent of aggregation in an RBC suspension is determined by both the composition of the suspending medium (e.g., protein or polymer size and concentration, pH, ionic strength, and so forth, see Ref. 34) and by the properties of the RBC (27, 31). Two theories have been proposed for the mechanism(s) involved in RBC aggregation (27): *1*) the bridging model in which increased surface adsorption of proteins or other macromolecules leads to increased aggregation and *2*) the depletion model in which the protein or polymer concentration at the RBC surface is less than the bulk phase and an osmotic gradient draws fluid away from gaps between cells, thus leading to aggregation (40). In this latter model, less adsorption on the RBC surface would favor greater aggregation. Neither

Downloaded from http://ajpheart.physiology.org/ by 10.220.33.1 on October 18, 2017

model for RBC aggregation excludes the contribution of cellular factors to RBC aggregation (31).

The degree or extent of RBC aggregation has been traditionally viewed in terms of an energy balance between aggregating and disaggregating forces, where aggregating forces are related to the concentration and properties of specific macromolecules (e.g., fibrinogen and dextran) and thus the magnitude of bridging energy (or osmotic gradient), whereas disaggregating forces include fluid shear stress, membrane-based electrostatic repulsive forces, and RBC membrane strain energy (11, 12). RBC membrane properties can thus be expected to affect aggregating forces via influencing the surface concentration of macromolecules and the contact area between cells and also to affect disaggregating forces. Therefore, the above-mentioned relations between RBC aggregation in plasma and in a defined polymer solution must involve the effects of one or more cellular properties that still remain to be fully defined. Currently, however, RBC membrane surface charge and RBC membrane mechanical behavior are the most commonly considered biophysical properties of RBC vis-à-vis their aggregation behavior (12, 27).

Comparative analyses of RBC membrane lipids have revealed species-specific differences in phospholipid composition (35), and our SDS-PAGE results (Fig. 8) imply that significant differences may exist in the structure of carbohydrate-rich proteins that are the main carriers of RBC negative surface charge. The two-phase partitioning results obtained herein (Fig. 7) revealed that horse, human, and rat RBC have different partition coefficients, suggesting a difference in membrane surface charge (43) with the order being rat $>$ human $>$ horse. As discussed above, a lower surface charge would be expected to favor RBC aggregation by reducing electrostatic repulsive forces; the greater aggregation tendency of horse RBC could thus be associated with their lower surface charge.

Literature reports regarding the surface charge of RBC from different species are not in total agreement: *1*) Seaman and Uhlenbruck (36) calculated surface charge based on electrophoretic mobility measurements and reported a slightly higher charge for horse versus human RBC, and *2*) in contrast, Walter and Widen (44) reported slightly lower partition coefficients for horse RBC versus human RBC in a charge-sensitive two-phase polymer system. They also reported that horse RBC had significantly lower partition coefficients in a non-charge-sensitive two-phase system, which is known to be sensitive to the membrane ratio of poly- to monounsaturated fatty acids (44). Rat RBC membranes have a very high ratio of poly- to monounsaturated fatty acids and have a high partition coefficient in non-charge-sensitive two-phase systems (44). Our results (Fig. 7) indicate that rat RBC also have a high partition coefficient in a charge-sensitive two-phase system, thus suggesting a high surface charge that may be responsible for their low aggregation tendency. Although these findings seem to suggest some degree of uncertainty regarding the relationships among partition coefficients, electrophoretic mobility, and RBC surface charge, it is notable that almost all mobility measurements are made in protein- or polymer-free buffers, whereas partition coefficients are determined in aqueous polymer systems. However, there are literature reports of RBC mobility in buffer versus protein or polymer solutions: *1*) young and old human RBC have identical mobilities in PBS yet exhibit significant differences (old $>$ young) when tested in plasma, serum, or dextran 70 (38), and *2*) Walter and Widen (45) also report differences between RBC mobilities in buffer versus polymer solutions and suggest the importance of mobility studies in polymer systems relevant to the RBC characteristics being investigated (e.g., aggregability).

The cellular and membrane mechanical properties of RBC have also been reported to be different in various species (2, 46). Amin and Sirs (2) reported that horse RBC were extremely deformable and that this property could be related to the high aggregation tendency of horse RBC. The cell must deform to form parallel surfaces during aggregation; hence, if RBC are more deformable, their aggregation will be enhanced (37). Conversely, our ektacytometry results (Fig. 5) imply that horse RBC may have significantly lower deformability versus human RBC, since both the change in EI in response to shear stress and the maximum deformation index were markedly lower for horse RBC. However, it is notable that Amin and Sirs (2) employed a sedimentation-centrifugal packing method to assess RBC deformability, suggesting that results with this method could be affected by RBC aggregation and thus may not solely reflect RBC deformability.

The ektacytometer results in our study (Fig. 5) require evaluation in terms of possible differences in behavior of different RBC in a fluid shear field and in terms of the manner in which EI-shear stress data are interpreted. At the lowest shear stress employed (0.5 Pa), both horse and rat RBC had higher EI compared with human RBC. It is also obvious from Fig. 5 that, compared with human RBC, maximal deformation was observed at lower shear stresses for rat and horse RBC and that the maximum EI was smaller for both nonhuman species. Although it has been previously reported that an artifact can occur when using small RBC with older-type ektacytometers that employ paired diodes as detectors (22), the video camera-computer image analysis system of the LORCA obviates this source of error (19). Nevertheless, interpretation of EI-shear stress curves for RBC from different species is still somewhat problematic. The lower shear stress necessary for maximum deformation may suggest a higher "deformability" for horse and rat RBC. Alternatively, the smaller increase of EI between low and high shear stress for horse and rat RBC might be considered to reflect a lower degree of deformability. Because the absolute values of EI are affected by cell orientation as well as by cell deformation (19), it might be suggested that the change of EI in response to shear stress would be a more appropriate measure of deformability. From this point of view, rat and horse RBC seem to have a similar deformability that is lower than human RBC (Fig. 5).

Downloaded from http://ajpheart.physiology.org/ by 10.220.33.1 on October 18, 2017

Shape recovery t_c for rat, and especially horse, RBC was also lower compared with human RBC (Fig. 6). Because this t_c is proportional to the ratio of RBC membrane surface viscosity to RBC membrane shear elastic modulus (20), this ratio for horse RBC is markedly less than for human cells. Note that, at the levels used in the present study, dextran has no effect on either the membrane surface viscosity or shear elastic modulus of human RBC (30, 41); similar data for horse or rat RBC do not appear to exist. It has been observed that cross-linking agents induce decreases of both t_c and RBC deformability (5) and that *band 4.2* protein can competitively inhibit the cross-linking activity of RBC transglutaminases (39). The absence of the expected high-molecular-weight aggregates in the gels (Fig. 8) may indicate that the cross-links are disrupted during sample preparation or that *band 4.2* has some other role. *Band 4.2* is generally accepted as a stabilizing component of the RBC membrane, and a deficiency of this protein is characterized by spherocytosis and increased membrane fragility (13, 49); horse RBC are known to have a high tendency to form echinocytes (47), suggesting a lower shape stability.

Given the absence of a Coomassie blue-stained band in the 4.2 region for horse RBC membrane proteins (Fig. 8), it is possible that horse RBC may have a higher shear modulus and hence a reduced t_c. Such a suggestion is, however, speculative, since direct experimental measures of horse RBC membrane shear elastic modulus do not appear to exist.

From the above discussion, it is obvious that our current knowledge of RBC biophysical and physicochemical properties cannot, as yet, provide a satisfactory basis to explain differences in aggregability of RBC from various species. However, the observed species-specific aggregation characteristics are most likely related to differences in the manner in which macromolecules interact with the RBC surface, which is in turn affected by the specific surface structure of RBC. It has been proposed that *band 3*, the major transmembrane protein of the RBC membrane, might be the binding site for macromolecules involved in the aggregation process (15). Our SDS-PAGE analysis revealed no significant differences in *band 3* among horse, human, and rat RBC membranes, but all three species did exhibited unique periodic acid-Schiff-stained band patterns (Fig. 8). These periodic acid-Schiff-stained, carbohydrate-rich proteins are also known to have extensive surface exposure, thus providing binding sites for many biological molecules (10). Detailed analysis of these proteins and their interactions with aggregating macromolecules (e.g., fibrinogen and dextran) may provide important information relevant to the mechanisms involved in RBC aggregation.

We thank Dr. Mahmoud Razavian for help with the aqueous two-phase polymer partitioning studies of the various red blood cell populations and Dr. Aysegul Temiz and Rose Wenby for technical support. Additional thanks for comfort, encouragement, and support are extended to E. Baskurt and D. Meiselman.

This work was supported by an International Scholar Award from the J. William Fulbright Foreign Scholarship Board (to O. K. Baskurt) and by National Institutes of Health Research Grants HL-15722 (to H. J. Meiselman), HL-48484 (to H. J. Meiselman), and GM-28673 (to R. A. Farley).

Address for reprint requests: H. J. Meiselman, Dept. of Physiology and Biophysics, USC School of Medicine, 1333 San Pablo St., MMR 626, Los Angeles, CA 90033.

Received 19 May 1997; accepted in final form 7 August 1997.

REFERENCES

1. **Allen, B. V.** Relationships between the erythrocyte sedimentation rate, plasma proteins and viscosity, and leucocyte counts in thoroughbred racehorses. *Vet. Rec.* 122: 329–332, 1988.
2. **Amin, T. M., and J. A. Sirs.** The blood rheology of man and various animal species. *Q. J. Exp. Physiol.* 70: 37–49, 1985.
3. **Andrews, F. M., N. L. Korenek, W. L. Sanders, and R. L. Hamlin.** Viscosity and rheologic properties of blood from clinically normal horses. *Am. J. Vet. Res.* 53: 966–970, 1992.
4. **Baskurt, O. K.** Deformability of red blood cells from different species studied by resistive pulse shape analysis technique. *Biorheology* 33: 169–179, 1996.
5. **Baskurt, O. K., and H. J. Meiselman.** Determination of red blood cell shape recovery time constant in a Couette system by the analysis of light reflectance and ektacytometry. *Biorheology* 33: 489–503, 1996.
6. **Baskurt, O. K., A. Temiz, and H. J. Meiselman.** Red blood cell aggregation in experimental sepsis. *J. Clin. Lab. Med.* 130: 183–190, 1997.
7. **Bauersachs, R. M., R. B. Wenby, and H. J. Meiselman.** Determination of specific red blood cell aggregation indices via an automated system. *Clin. Hemorheol.* 9: 1–25, 1989.
8. **Bull, B. S., and J. D. Brailsford.** The zeta sedimentation rate. *Blood* 40: 550–557, 1974.
9. **Cabel, M., H. J. Meiselman, A. S. Popel and P. C. Johnson.** Contribution of red blood cell aggregation to venous vascular resistance in skeletal muscle. *Am. J. Physiol.* 272 (*Heart. Circ. Physiol.* 41): H1020–H1032, 1997.
10. **Chasis, J. A., and N. Mohandas.** Red blood cell glycophorins. *Blood* 80: 1869–1879, 1992.
11. **Chien, S.** Biophysical behavior of red cells in suspensions. In: *The Red Blood Cell*, edited by D. M. Surgenor. New York: Academic, 1975, p. 1031–1133.
12. **Chien, S., and L. A. Sung.** Molecular basis of red cell membrane rheology. *Biorheology* 27: 327–344, 1990.
13. **Cohen, C. M., E. Dotimas, and C. Korsgren.** Human erythrocyte membrane protein band 4.2 (Pallidin). *Semin. Hematol.* 30: 119–137, 1993.
14. **Elsner, R., and H. J. Meiselman.** Splenic oxygen storage and blood viscosity in seals. *Marine Mammal Science* 11: 93–96, 1993.
15. **Fabry, T. L.** Mechanism of erythrocyte aggregation and sedimentation. *Blood* 70: 1572–1576, 1987.
16. **Fairbanks, G., T. L. Steck, and D. F. H. Wallach.** Electrophoretic analysis of the major polypeptide of the human erythrocyte membrane. *Biochemistry* 10: 2606–2617, 1971.
17. **Gascoyne, S. C., and C. M. Hawkey.** Patterns of variation in vertebrate haematology. *Clin. Hemorheol.* 12: 627–637, 1992.
18. **Hakim, T. S., and A. S. Macek.** Effect of hypoxia on erythrocyte deformability in different species. *Biorheology* 25: 857–868, 1988.
19. **Hardeman, M. R., P. T. Goedhart, J. G. G. Dobbe, and K. P. Lettinga.** Laser-assisted optical rotational cell analyzer (LORCA). 1. A new instrument for measurement of various structural hemorheological parameters. *Clin. Hemorheol.* 14: 605–618, 1994.
20. **Hochmuth, R. M., P. R. Worthy, and E. A. Evans.** Red cell extensional recovery and the determination of membrane viscosity. *Biophys. J.* 26: 101–114, 1979.
21. **Johnn, H., C. Phipps, S. C. Gascoyne, C. Hawkey, and M. W. Rampling.** A comparison of the viscometric properties of the blood from a wide range of mammals. *Clin. Hemorheol.* 12: 639–647, 1992.
22. **Johnson, R. M.** Ektacytometry of red blood cells. *Methods Enzymol.* 173: 35–54, 1989.

Downloaded from http://ajpheart.physiology.org/ by 10.220.33.1 on October 18, 2017

23. **Kumaravel, M., and M. Singh.** Sequential analysis of aggregation process of erythrocytes of human, buffalo, cow, horse, goat and rabbit. *Clin. Hemorheol.* 15: 291–304, 1995.
24. **Laemmli, U. K.** Cleavage of structural proteins during the assembly of the head of bacteriophage T4. *Nature* 227: 680–685, 1970.
25. **Lowe, G. D. O., and J. C. Barbanel.** Plasma and blood viscosity. In: *Clinical Blood Rheology*, edited by G. D. O. Lowe. Boca Raton, FL: CRC, 1988, p. 1–10.
26. **Meiselman, H. J.** Rheology of shape-transformed human red cells. *Biorheology* 15: 225–237, 1978.
27. **Meiselman, H. J.** Red blood cell role in RBC aggregation: 1963–1993 and beyond. *Clin. Hemorheol.* 13: 575–592, 1993.
28. **Meiselman, H. J., M. A. Castellini, and R. Elsner.** Hemorheological behavior of seal blood. *Clin. Hemorheol.* 12: 657–675, 1992.
29. **Mohandas, N., and E. A. Evans.** Mechanical properties of the red cell membrane in relation to molecular structure and genetic defects. *Annu. Rev. Biophys. Biomol. Struct.* 23: 787–818, 1994.
30. **Nash, G. B., and H. J. Meiselman.** Effects of dextran and polyvinylpyrrolidone on red cell geometry and membrane elasticity. *Ann. NY Acad. Sci.* 416: 255–262, 1984.
31. **Nash, G. B., R. Wenby, S. O. Sowemimo-Coker, and H. J. Meiselman.** Influence of cellular properties on red cell aggregation. *Clin. Hemorheol.* 7: 93–108, 1987.
32. **Ohta, K., F. Gotoh, M. Tomita, N. Tanahashi, M. Kobari, T. Shinohara, Y. Tereyama, B. Mihara, and H. Takeda.** Animal species differences in erythrocyte aggregability. *Am. J. Physiol.* 262 (*Heart Circ. Physiol.* 31): H1009–H1012, 1992.
33. **Popel, A. S., P. C. Johnson, M. V. Kameneva, and M. A. Wild.** Capacity for red blood cell aggregation is higher in athletic mammalian species than in sedentary species. *J. Appl. Physiol.* 77: 1790–1794, 1994.
34. **Rampling, M. W.** Red cell aggregation and yield stress. In: *Clinical Blood Rheology*, edited by G. D. O. Lowe. Boca Raton, FL: CRC, 1988, p. 45–64.
35. **Roelofsen, B., G. Van Meer, and J. A. F. Op Den Kamp.** The lipids of red cell membranes. *Scand. J. Clin. Lab. Invest.* 41, *Suppl.* 156: 111–115, 1981.
36. **Seaman, G. V. F., and G. Uhlenbruck.** The surface structure of erythrocytes from some animal sources. *Arch. Biochem. Biophys.* 100: 493–502, 1963.
37. **Shiga, T., N. Maeda, and K. Kon.** Erythrocyte rheology. *Crit. Rev. Oncol. Hematol.* 10: 9–48, 1990.
38. **Sowemimo-Coker, S. O., P. Whittingstall, L. Pietsch, R. M. Bauersachs, R. B. Wenby, and H. J. Meiselman.** Effects of cellular factors on the aggregation behavior of human, rat and bovine erythrocytes. *Clin. Hemorheol.* 9: 723–737, 1989.
39. **Sung, L. A., S. Chien, Y. S. Fan, C. C. Lin, K. Lambert, L. Zhu, J. S. Lam, and L. S. Chang.** Human erythrocyte protein 4.2: isoform expression, differential splicing and chromosomal assignment. *Blood* 79: 2763–2770, 1992.
40. **Thomas, N. E., and W. T. Coakley.** Localized contact formation by erythrocyte membranes: electrostatic effects. *Biophys. J.* 69: 1387–1401, 1995.
41. **Tran-Son-Tay, R., G. B. Nash, and H. J. Meiselman.** Effects of dextran and membrane shear rate on red cell membrane viscosity. *Biorheology* 22: 335–340, 1985.
42. **Usami, S., S. Chien, and M. I. Gregersen.** Viscometric characteristics of blood of the elephant, man, dog, sheep and goat. *Am. J. Physiol.* 217: 884–890, 1969.
43. **Walter, H.** Surface properties of cells reflected by partitioning: red blood cells as a model. In: *Partitioning in Aqueous Two-Phase Systems*, edited by H. Walter, D. E. Brooks, and D. Fisher. Orlando, FL: Academic, 1985, p. 327–376.
44. **Walter, H., and K. E. Widen.** Immobilized metal ion affinity partitioning of erythrocytes from different species in dextran-poly(ethylene glycol) aqueous systems. *J. Chromatogr. Sci.* 641: 279–289, 1993.
45. **Walter, H., and K. E. Widen.** Cell partitioning in two-phase aqueous phase systems and cell electrophoresis in aqueous polymer solutions. Human and rat young and old red blood cells. *Biochim. Biophys. Acta* 1194: 131–137, 1994.
46. **Waugh, R. E.** Red cell deformability in different vertebrate animals. *Clin. Hemorheol.* 12: 649–656, 1992.
47. **Weiss, D. J., R. J. Geor, and C. M. Smith.** Effect of echinocytosis on hemorheologic values and exercise performance in horses. *Am. J. Vet. Res.* 55: 204–210, 1994.
48. **Windberger, U., V. Ribitsch, K. L. Resch, and U. Losert.** The viscoelasticity of blood and plasma in pig, horse, dog, ox, and sheep. *J. Exp. Anim. Sci.* 36: 89–95, 1994.
49. **Yawata, Y.** Red cell membrane protein band 4.2: phenotypic, genetic and electron microscopic aspects. *Biochim. Biophys. Acta* 1204: 131–148, 1994.

Downloaded from http://ajpheart.physiology.org/ by 10.220.33.1 on October 18, 2017